Carbohydrate Polymers 84 (2011) 756–761

Contents lists available at ScienceDirect

Carbohydrate Polymers

journal homepage: www.elsevier.com/locate/carbpol

The storage stability of chitosan/tripolyphosphate nanoparticles in a phosphate buffer

Min-Lang Tsai*, Rong-Huei Chen, Shi-Wei Bai, Wei-Yu Chen

Department of Food Science, National Taiwan Ocean University, 2 Pei-Ning Road, Keelung 20224, Taiwan

ARTICLE INFO

Article history:
Received 1 October 2009
Received in revised form 9 March 2010
Accepted 20 April 2010
Available online 29 April 2010

Keywords:
Chitosan
Tripolyphosophate
Nanoparticle
Particle size
Storage stability

ABSTRACT

The objective of this study is to investigate the effect of initial size and pH of the solution on the changes in size of chitosan/tripolyphosphate (CS/TPP) nanoparticles stored in a phosphate buffer at 25 °C. The size decreased with increasing pH of the storage phosphate buffer. The initial sizes of the nanoparticles themselves also affected storage stability—the larger ones decreased in size, however the smaller ones increased their size in a phosphate buffer with a pH of 7.5 at 25 °C for 10 days due to protonation or deprotonation effects on the chitosan molecules. The changes of nanoparticle sizes are classified into instantaneous, aging, and swelling/aggregation stages over the storage time of 97 days. Mechanisms for these size changes are discussed.

1. Introduction

Chitosan (CS) is a high molecular weight polysaccharide linked by a β-1,4 glycoside and is composed of *N*-acetyl-glucosamine and glucosamine. It is considered to be the most widespread polycationic biopolymer, as well as having non-toxic, biocompatible, biodegradable characteristics. CS can be applied in food processing, agriculture, biomedicine, biochemistry, wastewater treatment, membranes, microcapsules, nanoparticles, liquid crystalline material, etc. (Chang, Chang, & Tsai, 2007; Rinaudo, 2006; Tsai, Bai, & Chen, 2008).

The CS nanoparticle has attracted great attention in pharmaceutical applications including being targeted for colon or mucosal delivery, cancer therapy, or delivery of vaccines, genes, antioxidants, etc. because the primary amine groups render a positive charge and mucoadhesive properties that make CS very useful in drug delivery applications (Agnihotri, Mallikarjuna, & Aminabhavi, 2004; Hu et al., 2008; Jang & Lee, 2008; Sarmento, Ferreira, Veiga, & Ribeiro, 2006; Vila et al., 2004; Yuan, Li, & Yuan, 2006). A CS nanoparticle is a very efficient and non-toxic absorption enhancer for both orally and nasally administered peptide drugs (van der Lubben, Verhoef, Borchard, & Junginger, 2001). Moreover, preliminary blood compatibility tests for the acylated CS nanoparticle showed that the long aliphatic and aromatic acyl groups did not significantly influence the hemolytic activity and blood clotting behavior (Lee, Powers, & Baney, 2004). Furthermore, the potential use of polymeric nanoparticles as drug carriers has led to the development of many different colloidal delivery vehicles. The main advantages of this kind of system lies in its capacity to cross biological barriers, to protect macromolecules such as peptides, proteins, oligonucleotides, and genes from degradation in biological media, and to deliver drugs or macromolecules to a target site following a controlled release (López-León, Carvalho, Seijo, Ortega-Vinuesa, & Bastos-González, 2005). Moreover, the CS, *O*-carboxymethyl and *N*,*O*-carboxymethyl CS nanoparticle had a low cytotoxicity for breast cancer cells-MCF-7 and good antibacterial activity for *Staphylococcus aureus* (Anitha et al., 2009).

Desai, Labhasetwar, Walter, Levy, and Amidom (1997) reported that particle uptake by caco-2 cells depends significantly upon the particles diameter. The 100 nm diameter particles had a 2.5-fold greater uptake on a weight basis than the 1 μm and a 6-fold greater uptake than the 10 μm diameter particles. Similarly, in terms of number, the uptake of 100 nm diameter particles was 2.7×10^3 fold greater than the 1 μm and 6.7×10^6 fold greater than the 10 μm diameter particles.

Hanus, Hartzler, and Wagner (2001) reported that for four acrylic latex suspensions of fixed surface chemistry but varying particle size (radius 57–167 nm), aggregation rates increased with added salt for each particle size sample and with decreasing particle size sample for a given salt concentration.

The ionotropic gelation method is commonly used to prepare CS nanoparticles. In acidic solution, the $-NH_2$ of a CS molecule is protonized to be $-NH_3^+$, it interacts with an anion such as tripolyphosphate (TPP) by ionic interaction to form microgel parti-

* Corresponding author. Tel.: +886 2 2462 2192x5122; fax: +886 2 2463 4203.
E-mail address: tml@mail.ntou.edu.tw (M.-L. Tsai).

0144-8617/$ – see front matter © 2010 Elsevier Ltd. All rights reserved.
doi:10.1016/j.carbpol.2010.04.040

cles (Lee, Mi, Shen, & Shyu, 2001). This method is very simple and mild. In addition, reversible physical cross-linking by electrostatic interaction, instead of chemical cross-linking, is applied to prevent possible toxicity of reagents and other undesirable effects (Shu & Zhu, 2000).

It is very important in usages of CS nanoparticles with consistent characteristics such as the size of suspension in solution over long periods of time. Tang, Huang, and Lim (2003) reported that turbid sediments were formed with substantial swelling of CS/TPP nanoparticles suspended in water at room temperature over 3 weeks. TEM micrographs associated the turbidity with a growth in the particle mean size, possibly contributed to by an inflow of water into the nanoparticles by osmosis due to the presence of TPP. This caused the nanoparticles to expand and the polymer matrix to fracture. López-León et al. (2005) reported that the CS/TPP nanogel particles were stored at 5 and 20 °C in a non-buffer solution (pH 5–6) containing 1 mM of KBr. The average diameters and standard deviations of CS nanoparticles increased with time. The average diameters and standard deviations increase significantly due to swelling and spontaneous disintegration after 15 and 7 days for 5 and 20 °C samples, respectively. They suggested that CS/TPP nanogel behaved as a metastable system. However, Gan, Wang, Cochrane, and McCarron (2005) showed the size growth kinetics of CS/TPP nanoparticles. Ionic gelation and growth of the nanoparticles were completed within the first hour and then there was a slight increase in particle size from about 180 to 240 nm over the next 24 h. They considered that no apparent aggregation of particles was observed during this period at 20 °C in pH 5.0.

The storage stability of CS/TPP was no more than 3 weeks as reported in the above-mentioned literatures. Storage stability after 3 weeks will limit their applications. Nanoparticle expansion and polymer matrix fracture could result in an inflow of water into the nanoparticles by osmosis due to the presence of TPP. Could the properties of the storage solution, such as increasing the salt concentration (Hanus et al., 2001) and/or controlling a proper initial size of CS/TPP, be manipulated to improved storage stability in order to extend the shelf-life for future application of CS/TPP nanoparticles? The objective of this study is to investigate the effect of different initial sizes of CS/TPP nanoparticles and storage conditions, especially a solution's pH, on storage stability in a phosphate buffer of pH 7.5 at 25 °C for a long period of time, and to propose conditions for the manipulation of the size of nanoparticles during storage.

2. Experimental

2.1. Materials

Squid (*Illex Argentinus*) pens were donated as a gift from Shin Dar Bio-Tech. Co. Ltd (Taoyuan, Taiwan). Tripolyphosphate pentasodium, acetic acid, sodium acetate, sodium azide, and potassium bromide were purchased from Sigma–Aldrich (USA). Hydrochloric acid and sodium hydrogen carbonate were purchased from Merck (Germany).

2.2. Preparation of chitosan

The squid pens were ground to a 40–60 mesh size. Each 100 g of powder was immersed in 500 mL of 1 M hydrochloric acid solution overnight. The powder was washed to neutrality and drained. The powder was soaked in 500 mL of 2 M sodium hydroxide at an ambient temperature overnight, and then soaked in 500 mL of 2 M sodium hydroxide solution at 100 °C for 4 h, washed and dried to produce about 35 g of β-chitin (Tsai et al., 2008). β-Chitin was added to a 50% (w/w) sodium hydroxide solution at a ratio of 1 (g solid):20 (mL solution). The deacetylation reaction took place at 100 °C for 1 h. Then the CS was washed to neutrality and freeze-dried (Tsai et al., 2008).

2.3. Measurement of degree of deacetylation of CS

Infrared spectrometry was used to determine the degree of deacetylation (DD) of the CS (Baxter, Dillon, Taylor, & Roberts, 1992). CS powder was sieved through a 200 mesh then mixed with KBr (1:100) and pressed into a pellet. The absorbances of amide 1 (1655 cm^{-1}) and of the hydroxyl band (3450 cm^{-1}) were measured using a Bio-Rad FTS-155 infrared spectrophotometer (USA). The band of the hydroxyl group at 3450 cm^{-1} was used as an internal standard to correct for disc thickness and for differences in CS concentration in making the KBr disc. The percentage of the amine group's acetylation in a sample is given by $(A_{1655}/A_{3450}) \times 115$. Here, A_{1655}, A_{3450} are the absorbances at 1650 and 3450 cm^{-1}, respectively. CS with a DD of 71% was used in this study.

2.4. Determination of molecular weight of CS

Size exclusion high-performance liquid chromatography (SE-HPLC) method of Tsaih and Chen (1999) was followed. A column (7.8 mm × 30 cm) packed with TSK gel $G4000_{XL}$ and G5000 PW_{XL} (Tosoh Co. Ltd, Japan) was used. The mobile phase consisted of 0.2 M acetic acid/0.1 M sodium acetate, and 0.008 M sodium azide. Sample concentration of 0.1% (w/v) was loaded and eluted with a flow rate of 0.6 mL/min by an LDC Analytical ConstaMetric 3500 pump. The elute peak was detected by an RI detector (Gilson model M132, USA). The data were analyzed by a Chem-Lab software (SISC, Taiwan). CSs with known molecular weight (determined by light scattering) were used as markers. The calibration curve of elution volume and molecular weight was established. The weight average molecular weights of the samples were calculated from the calibration curve with the Chem-Lab software. CS with a molecular weight of 450 kDa was used in this study.

2.5. Preparation of nanoparticles

Different concentrations of CS solutions (1, 2, 4, and 10 mg/mL) with 1% (w/w) acetic acid, and pH ca. 4.5, were prepared, then, a TPP solution (0.84 mg/mL) was added to the CS solution at a volume ratio of 5:2 (v/v) (CS:TPP). The solution was treated with ultrasonic radiation (VCX 750, Sonic & Materials, Inc., USA). After treatment, a 5-fold volume phosphate buffer (pH 5.5, 7.5, and 9.9) was added into the CS/TPP solution. Larger particles were removed by 12,000 × *g* centrifugal treatment. The supernatant containing the CS/TPP nanoparticles was harvested and the mean diameter was determined by light scattering. The ultrasonic radiation powers exerted were 10, 29, and 48 W; for 1, 2, and 4 min; at 4, 25, and 45 °C (Tsai et al., 2008).

2.6. Measure particle size of nanoparticle

CS nanoparticles in 3 mL solutions contained inside a sample tube were detected by a dynamic light scattering system (Malvern 4700, Malvern Instrument, UK) radiating an incident light with a wavelength of 632.8 nm to measure the intensity of the scattered light at an angle of 90° under the temperature of 30 ± 0.1 °C. Through the intensity of scattered light transferred into the diffusion factor, the mean value was obtained by each 10-scan measurement which was repeated three times. As shown below, the particle size of nanoparticles was computed by the Stoke-Einstein formula (Banerjee, Mitra, Singh, Sharma, & Maitra, 2002)$R = \frac{KT}{6\pi\eta D}$ where R is the radius of the particle (m), K is the

Table 1
The changes of mean diameter (nm) of CS/TPP nanoparticles during storage 10 days in pH 7.5 phosphate buffer at 25 °C.

Term	Prepared condition[a]	Storage time (day)					SB[b]	SA
		0	1	3	6	10		
A	29-1-4-25	92.7 ± 0.8^{b}	93.6 ± 1.1^{ab}	94.1 ± 0.3^{ab}	94.3 ± 0.2^{ab}	94.8 ± 0.8^{a}	0.18	0.35
B	29-2-4-45	112.7 ± 0.3^{d}	113.5 ± 0.1^{c}	114.7 ± 0.4^{b}	116.0 ± 0.4^{a}	116.4 ± 0.2^{a}	0.36	0.37
C	48-2-4-25	117.5 ± 0.7^{c}	118.9 ± 0.4^{b}	119.0 ± 0.2^{b}	119.3 ± 0.8^{b}	120.7 ± 1.2^{a}	0.26	0.42
D	29-2-4-25	127.8 ± 1.8^{a}	127.8 ± 1.2^{a}	128.4 ± 0.8^{a}	128.7 ± 1.5^{a}	128.3 ± 2.2^{a}	0.10	0.42
E	29-2-4-4	144.4 ± 2.5^{a}	141.1 ± 07^{b}	140.9 ± 0.1^{b}	140.6 ± 1.1^{b}	140.6 ± 0.5^{b}	−0.26	0.37
F	48-2-2-25	159.0 ± 0.6^{a}	157.5 ± 0.9^{b}	157.0 ± 0.8^{b}	156.6 ± 0.4^{b}	156.4 ± 1.0^{b}	−0.22	0.48
G	48-2-1-25	173.4 ± 1.4^{a}	170.1 ± 1.1^{b}	169.8 ± 0.9^{b}	169.2 ± 1.1^{b}	168.8 ± 2.1^{b}	−0.34	0.59
H	10-2-4-25	183.1 ± 0.5^{a}	178.9 ± 0.6^{b}	176.9 ± 1.2^{c}	176.5 ± 0.7^{c}	176.5 ± 0.2^{c}	−0.48	0.47
I	29-4-4-25	205.3 ± 0.5^{a}	202.8 ± 0.9^{b}	201.8 ± 0.8^{bc}	199.8 ± 1.1^{cd}	199.5 ± 1.3^{d}	−0.53	0.10
J	29-10-4-25	709.2 ± 1.7^{a}	701.4 ± 4.4^{b}	689.3 ± 6.1^{b}	676.7 ± 4.7^{c}	677.4 ± 4.9^{c}	−4.13	−0.87

Values are mean ± S.D. ($n = 3$). Different letters (a–d) in the same row indicate significant differences ($p < 0.05$) between samples.

[a] 29-1-4-25 expressed the CS/TPP nanoparticle was prepared with ultrasonic output power 29 W, 1 mg/mL CS solution, radiation time 4 min, solution temperature 25 °C. The rest may be deduced by analogy.

[b] SB and SA expressed the slopes of storage time versus nanoparticle mean diameter plots before and after 10 days, respectively.

Boltzmann constant (J/K), T is the absolute temperature (K), η is solution viscosity (cp), and D is the diffusion factor (m^2/s).

2.7. Measurement of the storage stability of nanoparticle

For the purpose of realizing changes in CS particle sizes of nanoparticles and the storage stability, the mean diameter of nanoparticles was used as the indicator to evaluate the storage stability of CS nanoparticles in a phosphate buffer (pH 5.5, 7.5, and 9.9) at 25 °C for a period of time prior to removal.

3. Results and discussion

3.1. Effect of preparation conditions on size of nanoparticles

Table 1 shows the effect of preparation conditions and storage periods on the changes of the mean diameter of CS/TPP nanoparticles in a pH 7.5 phosphate buffer at 25 °C for 10 days. The results indicate that the initial sizes of nanoparticles depend on ultrasonic output power, ultrasonic radiation time, solution temperature, and CS concentration. These results are similar to the results of Gan et al. (2005), Grenha, Seijo, and Remuñán-López (2005) and Tsai et al. (2008). This may be due to the size of nanoparticles, the molecular weight of the CS used, and/or concentration of the CS solution in the preparation. Smaller nanoparticles were prepared from CS with less molecular weight and/or a lower CS concentration. In contrast, larger sized nanoparticles were prepared from a higher molecular weight and/or higher CS concentration. The molecular weights of CS depended on ultrasonic output power, radiation time, solution temperature, etc. during ultrasonic treatment (Popa-Nita, Lucas, Ladaviè, David, & Domard, 2009; Tsaih & Chen, 2003; Tsaih, Tseng, & Chen, 2004), and the concentration of CS used (Tsaih et al., 2004).

The initial size of nanoparticles A, D, I, and J were 92.7, 127.8, 205.3, and 709.2 nm, respectively. The reasons for having different nanoparticle sizes might be solely due to different CS concentrations used in preparation solutions because other preparation conditions such as the ultrasonic output power, radiation time, and solution temperatures were identical. The CS concentration increased 2, 4, and 10 times, the initial size increased 1.4, 2.2, and 7.7 times for nanoparticles D, I, and J, respectively. The increase in the initial size of nanoparticle J was unusually large compared to increases in initial sizes of nanoparticle D and I. This may be because nanoparticle J formed a cluster due to the enormously high concentration used. The effect of CS concentration on the nanoparticle is similar to that previously described by Grenha et al. (2005). These authors reported that the zeta potential increased with increasing CS concentration when TPP concentration was fixed. However, the storage stability of nanoparticles may be related to zeta potential. This effect will be explored in a future study.

The effect of output power on the initial size of the resulting nanoparticles might be from the changes of the initial size of nanoparticles C, D, and H. The initial size of nanoparticles C, D, and H were 112.7, 127.8, and 183.1 nm, the output powers were 48, 29, and 10 W, respectively. Higher input power will result in smaller molecular weight chitosan and in turn will result in smaller initial sizes of CS/TPP nanoparticles (Cao, Zhang, & Huang, 2005; Tang et al., 2003; Tsai et al., 2008).

The effect of radiation time on the initial size of the resulting nanoparticle might be from the changes of the initial size of nanoparticles C, F, and G. The initial sizes of nanoparticles C, F, and G were 117.5, 159.0, and 173.4 nm, the radiation times were 4, 2, and 1 min, respectively. The longer radiation time will result in smaller molecular weight chitosan and in turn will result in smaller initial sizes of CS/TPP nanoparticles (Lan, Yang, & Li, 2004).

The effect of solution temperature on the initial size of resulting nanoparticles might be from the changes of the initial size of nanoparticles B, D, and E. The initial size of nanoparticles B, D, and E were 112.7, 127.8, and 144.4 nm, the solution temperatures were 45, 25, and 4 °C, respectively. The higher solution temperature will result in smaller molecular weight chitosan and in turn will result in smaller initial sizes of CS/TPP nanoparticles (Cao et al., 2005; Tsai et al., 2008).

3.2. Storage stability in 10 days

3.2.1. pH effect

The original size of the CS/TPP nanoparticle is 306.5 nm (Fig. 1) right after preparation with an ultrasonic output power of 29 W on 2 mg/mL CS solution for 4 min at 25 °C (i.e. nanoparticle D in Table 1). However, the sizes reduced to 160.6, 127.8, and 111.2 nm, respectively, after being transferred to phosphate buffer with a pH of 5.5, 7.5 and 9.9 for 1 h at 25 °C. Fig. 2 illustrates the effect the pH of the storage solutions had on the size of the CS/TPP nanoparticles. The results indicated that the size of the nanoparticles decreased with the increase of the solutions' pH levels. This may be due to the fact that the nanoparticles formed with CS and TPP are metastable nanogels. The structure of the nanoparticles was easily changed with different environment conditions such as the pH and ionic strength of the solutions (Gan et al., 2005; López-León et al., 2005; Yu, Hu, Pan, Yao, & Jiang, 2006). This phenomenon is due to the polycation property of CS. In lower pH solutions, CS molecules become more extended due to higher protonation and this leads to higher hydrodynamic volume nanoparticles. On the contrary, in higher pH solutions, the CS molecule shrinks due to lower protonation and/or

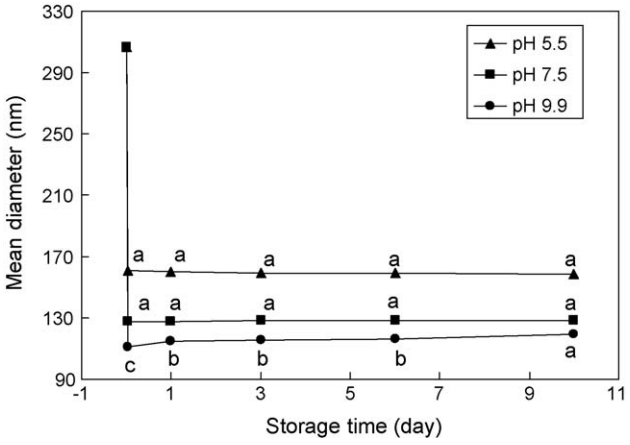

Fig. 1. Effect of pH (pH 5.5, 7.5 and 9.9) of storage solution and storage period on the changes of mean diameter of CS/TPP nanoparticles over time when stored at 25 °C. The nanoparticle was obtained by ultrasonic treatment on 2 mg/mL CS solution with 29 W for 4 min at 25 °C. (a–c) Values are mean ± S.D. (n = 3). Different letters in the same pH storage solution indicate significant differences (p < 0.05) between samples.

forms more inter- or intra-molecular hydrogen bonds, thus leading to smaller hydrodynamic volume nanoparticles.

3.2.2. Initial size effect

Table 1 shows the nanoparticles A–C with an initial size smaller than 120 nm. The size increased significantly with increasing storage time. But nanoparticle D, stored under the same conditions, increased slightly in size but not significantly with the increase in storage time. However, nanoparticles E-J, with particle sizes larger than 140 nm, showed trends of size changes different from nanoparticles A-D. The sizes of nanoparticles E-G decreased significantly in Day 1; nevertheless, the size decrease was insignificant with increasing storage time after Day 1. The particle size of nanoparticle H decreased significantly with increasing storage time before Day 3, nevertheless the size decreased was insignificant with increased storage time after that. The size of nanoparticle I decreased significantly with increasing storage time. In other words, the tendencies of size change of these nanoparticles were influenced with the initial mean diameter of the nanoparticle. The rate of the size changes of the nanoparticles was calculated from size changes versus storage time and was designated as SB (Table 1). Fig. 3 shows the relationship between the initial mean diameter of

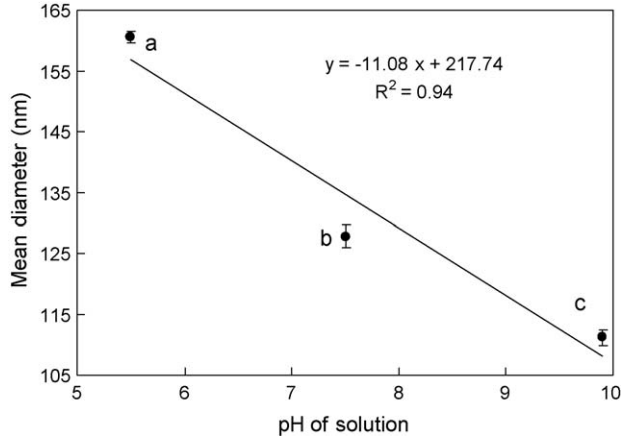

Fig. 2. pH of storage solution effect on the size of CS/TPP nanoparticles. (a–c) Values are mean ± S.D. (n = 3). Different letters indicate significant differences (p < 0.05) between samples. The CS/TPP nanoparticles were prepared at an ultrasonic radiation output power of 29 W upon 2 mg/mL CS solution for 4 min at 25 °C.

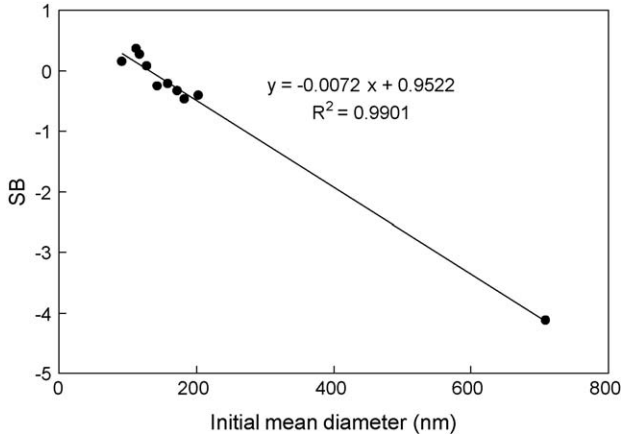

Fig. 3. The relationship between initial mean diameter of CS/TPP nanoparticles and the rate of size changes of nanoparticles (SB).

CS/TPP nanoparticles and the rate of size changes of nanoparticles (SB). The results in Fig. 3 show that those of initially larger size reduced particle size, while those of initially smaller size raised particle size in pH 7.5 phosphate buffer at 25 °C for 10 days. The nanoparticles with an initial size of about 132 nm, calculated from the equation in Fig. 3, did not vary when stored in the same solution conditions.

3.3. Long-term storage stability

Fig. 4 indicates that the mean diameter change of nanoparticle D stored in a phosphate buffer of pH 7.5 at 25 °C over a time of 97 days. Results in Fig. 4a show the slope of regression analysis for a short period (within 10 day, SB) and long period (10–97 days, SA) was 0.10 and 0.42, respectively. The SB and SA of other nanoparticles were listed in Table 1 too. The results indicate that the trends of mean diameter change may be varied, reflecting the different changes during different stages in long-term storage.

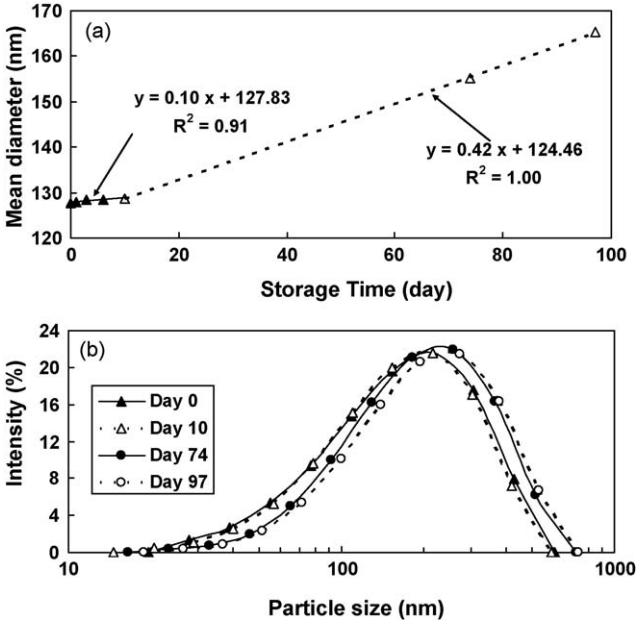

Fig. 4. (a) The slopes of storage time versus nanoparticle mean diameter within Day 10 (SB) and between Day 10 and Day 97 (SA) of CS/TPP nanoparticles a phosphate buffer with pH 7.5 at 25 °C over time. (b) Effect of storage time on the particle size distributions of CS/TPP nanoparticles. The nanoparticle was obtained by ultrasonic treatment on 2 mg/mL CS solution at 29 W for 4 min at 25 °C.

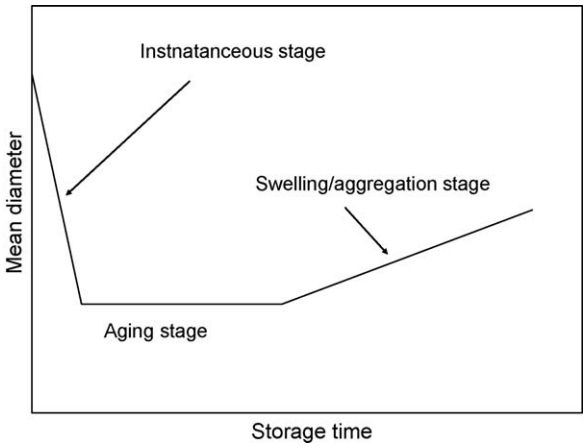

Fig. 5. Schematic diagram illustrates three stages of mean diameter variation of CS/TPP nanoparticles stored in phosphate buffer over time.

Fig. 4b shows that the particle size distributions of nanoparticle D were similar between Day 0 and Day 10, however, the particle size distributions of Day 74 and Day 97 were significantly shift to larger size region. All of these particle size distributions were monomodal.

3.4. Stages of particle size change

A general picture of changing sizes of different initial sized CS/TPP nanoparticles was shown in Fig. 1. The particle sizes reduced rapidly due to the change of environmental conditions (e.g. solution pH changed from about 4.5 to 7.5 due to deprotonation of chitosan molecules as they were transferred to storage solutions) (Gan et al., 2005; López-León et al., 2005; Yu et al., 2006). This stage of rapid particle size reduction is designated as the instantaneous stage (Fig. 5). The time span to finish the instantaneous stage depended on the size of the initial nanoparticle which in turn depended on the molecular weight of the chitosan and/or the concentration of chitosan solution used in preparation of the CS/TPP nanoparticles. This may be due to the larger initial size nanoparticles prepared with a CS of higher molecular weight and/or higher concentration of CS solution, having more intermolecular entanglement and inter/intra-molecular hydrogen bonding, rendering a stable nanogel thus needing longer time to change the size of the nanoparticle. In addition, larger initial sized nanoparticles had larger diameters and the diffusion or permeation of the storage solution into larger nanoparticles needed more time than that of the smaller ones.

The aging stage begins with the reorganization of intermolecular entanglement, as well as the syneresis, inter/intra-molecular hydrogen bonding formation, and new crystalline region formation (López-León et al., 2005; Tang et al., 2003). The size change was insignificant maybe due to the balance between the above-mentioned forces.

The third stage was swelling/aggregation of the nanoparticles. Swelling was possibly due to the inflow of water into the nanoparticles by osmosis in the presence of TPP. Swelling of nanoparticles will lead to the polymer matrix fracture (López-León et al., 2005; Tang et al., 2003). Aggregation might be due to collision and adhesion of nanoparticles during storage. This will be elaborated on more in Section 3.6.

Nanoparticles in Table 1 can be classified into 5 groups according to size change during storage. Group 1, including nanoparticles A, B, and C, went into a swelling/aggregation stage directly after being transferred into a storage solution due to their smaller sizes. Large surface area facilitates the storage solution being diffused into nanoparticles. Protonation of chitosan molecules caused the reorganization of constituent molecular. This rendered the sizes of these nanoparticles significantly increased with increasing storage time.

For Group 2 (nanoparticle D), the size was changed insignificantly before Day 10, then the size increased significantly between Day 10 and Day 97. This indicated that the nanoparticle D went into an aging stage in the initial 10 days and then into a swelling/aggregation stage after Day 10. This may be due to the size of nanoparticle D being larger than the nanoparticles of Group 1 and needing more time for the aging stage, i.e. the reorganization of intermolecular entanglement, as well as the syneresis, inter/intra-molecular hydrogen bonding formation, and new crystalline regions formation between the initial 10 days and the swelling and/or aggregation between Day 10 and Day 97.

In Group 3, including nanoparticles E, F, G, and H, due to their still larger size, they could not complete the instantaneous stage in Day 1 but took until Day 3. The size decreased slightly but insignificantly between Day 3 and Day 10. Then sizes increased significantly with long storage time.

The size of nanoparticle I (Group 4) was even larger than the nanoparticles of Group 3 (E, F, G, and H). The size of the nanoparticle decreased during the first 10 days, i.e. in the instantaneous stage, and then went into the aging stage over time for 97 days.

Group 5 (nanoparticle J) is a special case. It decreased in size significantly with the increased storage time over 97 days. The SB and SA of nanoparticle J were −4.13 and −0.87, respectively. The values are significantly smaller than other nanoparticles shown in Table 1. The data indicated that the rate of decreasing size of nanoparticle J was significantly faster than other nanoparticles. This may be due to the fact that nanoparticle J was formed as a cluster by groups of smaller nanoparticles. The rapid decrease in size might be due to the particle separated from the cluster during storage time.

3.5. Manipulation of storage stability

The CS/TPP nanoparticle prepared in conditions listed in Table 1 and then transferred to a phosphate buffer with pH 7.5, showed a better storage stability than those of Tang et al. (2003) and López-León et al. (2005). López-León et al. (2005) reported that the CS/TPP nanogel particles were stored at 5 and 20 °C in a non-buffer solution (pH 5–6) containing 1 mM of KBr. The average diameters and standard deviations of CS nanoparticles increased with time. The average diameters and standard deviations began to increase significantly due to swelling and spontaneous disintegration after 15 and 7 days, for 5 and 20 °C samples, respectively.

Either the preparation conditions or storage conditions, especially for metastable nanogel, can manipulate the size of CS/TPP nanoparticles (Gan et al., 2005; Tang et al., 2003; Tsai et al., 2008). The storage stability of CS/TPP nanoparticles can be manipulated to form a better interpenetrating polymer chain crosslink, a higher degree of polymer entanglement, and/or ionic interaction, etc. (López-León et al., 2005; Tang et al., 2003) to have a stronger network structure. Additionally, the storage conditions affect the storage stability, e.g. solution temperature, pH, ionic strength, etc. For example, the electrical state of the CS nanoparticle was affected by the pH and ionic strength of the storage solution. This caused particle swelling or shrinkage, depending on whether the electrical repulsions increased or decreased, respectively (López-León et al., 2005). Furthermore, the non-buffered solution was a low osmosis pressure solution. So, the water molecules get into the nanoparticles by osmosis due to the presence of TPP and cause nanoparticles' swelling and spontaneous disintegration (Tang et al., 2003). On the other hand, for nanoparticles in a buffer solution, the difference in osmosis pressure is smaller between the phosphate buffer and nanoparticle. This might result in a lower swelling effect giving better storage stability.

3.6. Aggregation effect

The size of CS/TPP nanoparticles increased with time during storage. The nanoparticle expansion and polymer matrix fracture in less than 3 weeks are possibly contributed to by an inflow of water into the nanoparticles by osmosis due to the presence of TPP (López-León et al., 2005; Tang et al., 2003). However, in this study, the sizes of nanoparticles A-H increased only about 30% over 97 days. In a pH 7.5 phosphate buffer at 25 °C nanoparticle D was most stable for 10 days. Whereas, nanoparticle I was most stable for 97 days. Based on the following observations, we proposed the small portion aggregation of nanoparticles during storage was another reason that caused the size increases. 1. The average diameters and standard deviations of CS nanoparticles studied in this report varied a little and smoothly with time (Table 1). 2. The particle size distributions of nanoparticles with different stored period were monomodal (Fig. 4b). 3. Difference in osmosis pressure of solutions and nanoparticles was small because the pH 7.5 phosphate buffer was used instead of a non-buffer solution (pH 5–6) containing 1 mM of KBr (López-León et al., 2005). 4. Brownian motion, due to small temperature variations during storage, enhanced the collision between nanoparticles and the viscoelastic properties of those nanogels, facilitated adhesion and in turn the aggregation formation thus increased the size in long-term storage (Chen & Liu, 2002; Shaw, 1992). However, the aggregation should be small portion; otherwise, the average size of nanoparticles will increase very rapidly (Hanus et al., 2001).

4. Conclusions

The initial sizes of CS/TPP nanoparticles were influenced with preparation conditions such as ultrasonic output power, radiation time, solution temperature, and CS concentration. The changes of nanoparticles' sizes are classified into instantaneous, aging, and swelling/aggregation stages over time for 97 days. The size reduced rapidly in the instantaneous stage. The size change was insignificant in the aging stage. The size increased significantly in the swelling/aggregation stage. Swelling of nanoparticles was attributed to an inflow of water into the nanoparticles by osmosis, due to the presence of TPP however, aggregation of small portion nanoparticles during storage was another reason that caused the size increases over time for 97 days. The size variation of nanoparticles during storage can be manipulated by varying initial nanoparticle sizes and storage conditions.

Acknowledgements

The authors wish to express their appreciation for the financial support from National Science Council, Republic of China (NSC 97-2313-B-019-007-MY3).

References

Agnihotri, S. A., Mallikarjuna, N. N., & Aminabhavi, T. M. (2004). Recent advances on chitosan-based micro- and nanoparticles in drug delivery. *Journal of Controlled Release*, *100*, 5–28.

Anitha, A., Divya Rani, V. V., Krishna, R., Sreeja, V., Selvamurugan, N., Nair, S. V., Tamura, H., & Jayakumar, R. (2009). Synthesis, characterization, cytotoxicity and antibacterial studies of chitosan, O-carboxymethyl and N,O-carboxymethyl chitosan nanoparticles. *Carbohydrate Polymers*, *78*, 672–677.

Banerjee, T., Mitra, S., Singh, A. K., Sharma, R. K., & Maitra, A. (2002). Preparation, characterization and biodistribution of ultrafine chitosan nanoparticles. *International Journal of Pharmaceutics*, *243*, 93–105.

Baxter, A., Dillon, M., Taylor, K. D. A., & Roberts, G. A. F. (1992). Improved method for i.r. determination of the degree of N-acetylation of chitosan. *International Journal of Biological Macromolecules*, *14*, 166–169.

Cao, L. Y., Zhang, C. B., & Huang, J. F. (2005). Influence of temperature, [Ca2+], Ca/P ratio and ultrasonic power on the crystallinity and morphology of hydroxyapatite nanoparticles prepared with a novel ultrasonic precipitation method. *Materials Letters*, *59*, 1902–1906.

Chang, J. S., Chang, K. L. B., & Tsai, M. L. (2007). Liquid-crystalline behavior of chitosan in malic acid. *Journal of Applied Polymer Science*, *105*, 2670–2675.

Chen, R. H., & Liu, C. S. (2002). Effect of recovery methods and conditions on the yield, solubility, molecular weight, and creep compliance of regenerated chitosan. *Journal of Applied Polymer Science*, *84*, 193–202.

Desai, M. P., Labhasetwar, V., Walter, E., Levy, R. J., & Amidom, G. L. (1997). The mechanism of uptake of biodegradable microparticles in caco-2 cells is size dependent. *Pharmaceutical Research*, *14*, 1568–1573.

Gan, Q., Wang, T., Cochrane, C., & McCarron, P. (2005). Modulation of surface charge, particle size and morphological properties of chitosan-TPP nanoparticles intended for gene delivery. *Colloids and Surfaces B: Biointerfaces*, *44*, 65–73.

Grenha, A., Seijo, B., & Remuñán-López, C. (2005). Microencapsulated chitosan nanoparticles for lung protein delivery. *European Journal of Pharmaceutical Sciences*, *25*, 427–437.

Hanus, L. H., Hartzler, R. U., & Wagner, N. J. (2001). Electrolyte-induced aggregation of acrylic latex. 1. Dilute particle concentrations. *Langmuir*, *17*, 3136–3147.

Hu, B., Pan, C., Sun, Y., Hou, Z., Ye, H., Hu, B., & Zeng, X. (2008). Optimization of fabrication parameters to produce chitosan-tripolyphosphate nanoparticles for delivery of tea catechins. *Journal of Agricultural and Food Chemistry*, *56*, 7451–7458.

Jang, K. I., & Lee, H. G. (2008). Stability of chitosan nanoparticles for L-ascorbic acid during heat treatment in aqueous solution. *Journal of Agricultural and Food Chemistry*, *56*, 1936–1941.

Lan, J., Yang, Y., & Li, X. (2004). Microstructure and microhardness of SiC nanoparticles reinforced magnesium composites fabricated by ultrasonic method. *Materials Science and Engineering A*, *386*, 284–290.

Lee, D.-W., Powers, K., & Baney, R. (2004). Physicochemical properties and blood compatibility of acylated chitosan nanoparticles. *Carbohydrate Polymers*, *58*, 371–377.

Lee, S. T., Mi, F. L., Shen, Y. J., & Shyu, S. S. (2001). Equilibrium and kinetic studies of copper(II) ion uptake by chitosan-tripolyphosphate chelating resin. *Polymer*, *42*, 1879–1892.

López-León, T., Carvalho, E. L. S., Seijo, B., Ortega-Vinuesa, J. L., & Bastos-González, D. (2005). Physicochemical characterization of chitosan nanoparticles: Electrokinetic and stability behavior. *Journal of Colloid and Interface Science*, *283*, 344–351.

Popa-Nita, S., Lucas, J.-M., Ladaviè, C., David, L., & Domard, A. (2009). Mechanisms involved during the ultrasonically induced depolymerization of chitosan: Characterization and control. *Biomacromolecules*, *10*, 1203–1211.

Rinaudo, M. (2006). Chitin and chitosan: Properties and applications. *Progress in Polymer Science*, *31*, 603–632.

Sarmento, B., Ferreira, D., Veiga, F., & Ribeiro, A. (2006). Characterization of insulin-loaded alginate nanoparticles produced by ionotropic pre-gelation through DSC and FTIR studies. *Carbohydrate Polymers*, *66*, 1–7.

Shaw, D. J. (1992). *Introduction to colloid and surface chemistry* (4th ed.). Oxford: Butterworth-Heinemann Ltd.

Shu, X. Z., & Zhu, K. J. (2000). A novel approach to prepare tripolyphosphate/chitosan complex beads for controlled release drug delivery. *International Journal of Pharmaceutics*, *201*, 51–58.

Tang, E. S. K., Huang, M., & Lim, L. Y. (2003). Ultrasonication of chitosan and chitosan nanoparticles. *International Journal of Pharmaceutics*, *265*, 103–114.

Tsai, M. L., Bai, S. W., & Chen, R. H. (2008). Cavitation effects versus stretch effects resulted in different size and polydispersity of ionotropic gelation chitosan-sodium tripolyphosohate nanoparticle. *Carbohydrate Polymers*, *71*, 448–457.

Tsaih, M. L., & Chen, R. H. (2003). The effect of degree of deacetylation of chitosan on the kinetics of ultrasonic degradation of chitosan. *Journal of Applied Polymer Science*, *90*, 3526–3531.

Tsaih, M. L., & Chen, R. H. (1999). Molecular weight determination of 83% degree of deacetylation chitosan with non-gaussian and wide range distribution by high-performance size exclusion chromatography and capillary viscometry. *Journal of Applied Polymer Science*, *71*, 1905–1913.

Tsaih, M. L., Tseng, L. Z., & Chen, R. H. (2004). Effects of removing small fragment with ultrafiltration treatment and ultrasonic conditions on degradation kinetics of chitosan. *Polymer Degradation and Stability*, *86*, 25–32.

van der Lubben, I. M., Verhoef, J. C., Borchard, G., & Junginger, H. E. (2001). Chitosan for mucosal vaccination. *Advanced Drug Delivery Reviews*, *52*, 139–144.

Vila, A., Sánchez, A., Janes, K., Behrens, I., Kissel, T., Vila Jato, J. L., & Alonso, M. J. (2004). Low molecular weight chitosan nanoparticles as new carriers for nasal vaccine delivery in mice. *European Journal of Pharmaceutics and Biopharmaceutics*, *57*, 123–131.

Yu, S., Hu, J., Pan, X., Yao, P., & Jiang, M. (2006). Stable and pH-sensitive nanogels prepared by self-assembly of chitosan and ovalbumin. *Langmuir*, *22*, 2754–2759.

Yuan, X. B., Li, H., & Yuan, Y. B. (2006). Preparation of cholesterol-modified chitosan self-aggregated nanoparticles for delivery of drugs to ocular surface. *Carbohydrate Polymers*, *65*, 337–345.